Results in Physics 12 (2019) 486–503

Contents lists available at ScienceDirect

Results in Physics

journal homepage: www.elsevier.com/locate/rinp

Effect of CNTs dispersion on electrical, mechanical and strain sensing properties of CNT/epoxy nanocomposites

Hamed Tanabi[a,b,*], Merve Erdal[a]

[a] Department of Mechanical Engineering, Middle East Technical University, Dumlupinar Blvd. No. 1, 06800 Cankaya, Ankara, Turkey
[b] Department of Mechanical Engineering, University of Turkish Aeronautical Association, Okul Sok No. 11, 06790 Etimesgut, Ankara, Turkey

ARTICLE INFO

Keywords:
Carbon nanotubes
CNT/epoxy nanocomposites
Electric conductivity
Strain sensor
Magnetization

ABSTRACT

The remarkable electrical and mechanical properties of carbon nanotubes (CNTs) render CNT-reinforced nanocomposites as potentially attractive materials for strain-sensing and monitoring purposes. The dispersion state of CNTs in polymeric matrix has a significant role on the physical and the mechanical properties of the resulting CNT reinforced nanocomposites. In this study, a series of experiments were designed to investigate the effect of dispersion process parameters and CNT concentration, as well as their interactions on electrical, mechanical and strain sensing properties of CNT/epoxy nanocomposites. Composite samples were produced under different CNT/resin dispersion conditions based on a design of experiments approach, and were characterized using tensile testing, conductivity measurements and micrography. Based on the results, two regression models were established to predict the electric conductivity and the tensile strength of the CNT/epoxy nanocomposites. The robustness and accuracy of the models were verified by implementing verification tests. It was found that the nanocomposites fabricated by dispersing of lower amount of CNT with high mixing speeds and long mixing times had improved sensory properties and were more suitable for strain sensing applications. The effect of post dispersion state on electrical conductivity was also investigated by curing nanocomposites into a magnetic field. A straight forward 2D percolation-based model was used to predict the electrical conductivity and piezoresistivity of the magnetized nanocomposites. Both Experimental and numerical results showed that the electric conductivity could be increased significantly with post dispersing of CNTs using magnetization.

Introduction

The remarkable properties of carbon fillers such as their high thermal and electrical conductivities [1–3], flame redundancy [4,5] coupled with their superior mechanical properties [6,7] render them potentially attractive fillers for advanced composites production. Among these, carbon nanotubes (CNTs) have gained considerable attention since minimal CNT loadings could provide significant electrical conductivity as well as improvement in mechanical properties of the produced nanocomposites [8,9].

The mechanical, electrical and thermal properties of nanocomposites strongly depend on the dispersion state of CNTs in polymer matrix [10–12]. The research on the effect of CNT addition on the mechanical properties of CNT/epoxy composite indicates that there is an optimum content of CNT above which there is a decrease in tensile strength and/or modulus of elasticity of the composite. This issue is due to non-effective dispersion of CNT in resin matrix and existence of high amount of agglomerated CNT particles [9,10,13]. Research also shows that the electrical conductivity of CNT filled nanocomposites for the same CNT concentration can vary with two orders of magnitude among the samples prepared using different dispersion techniques [14].

Ultra-sonication and/or shear mixing are commonly used for dispersing CNTs in epoxy matrix [11,15,16]. The existence of strong Van der Waals forces among CNTs and high tendency of CNTs to agglomerate [11,15] are some of the challenges that render the effective dispersing of CNTs in a polymer matrix a continuing research issue. Chemical treatment of CNTs [17,18], using chemical surfactants [19,20] and dilute solutions [21,22] have been found to ease the dispersing process but did not necessarily have a positive effect on the electrical conductivity of the final nanocomposites [23,24]. The shear mixing conditions during the preparation of the CNT/resin suspensions (for composite production) were found to be effective on composite electrical conductivities [24] and in some cases, improved the electrical percolation threshold by one order of magnitude [25].

Dispersion state of CNTs in epoxy matrix can also be modified before and/or during curing process. The application of electric and

* Corresponding author at: Department of Mechanical Engineering, Middle East Technical University, Dumlupinar Blvd. No. 1, 06800 Cankaya, Ankara, Turkey.
E-mail addresses: htanabi@thk.edu.tr (H. Tanabi), merdal@metu.edu.tr (M. Erdal).

https://doi.org/10.1016/j.rinp.2018.11.081
Received 9 February 2018; Received in revised form 23 November 2018; Accepted 23 November 2018
Available online 26 November 2018

magnetic fields is known as an effective approach to compel CNTs to align in a matrix [26]. The response of CNTs to magnetic field is strongly affected by the residual [27] or embedded catalysts [28]. Different synthesizing methods yield CNTs with different morphologies and different quantity of residual catalyst material. It was found that CNTs with remaining catalyst materials such as Fe and FeCo are more sensitive to the magnetic field [27]. The alignment of CNTs can improve the mechanical (fracture resistance [29] and tensile strength [26]) and physical (thermal [29] and electrical [30] conductivities) properties of nanocomposites in the direction of CNT orientation.

CNT reinforced composites have the potential to attain structural health monitoring capabilities by exploiting the variation of electrical conductivity and its relation to strain and/or damage within the nanocomposite [31,32]. The electrical conductivity depends on formation of electrically conductive pathways within the composite due to the presence of CNT. During the stretching of the nanocomposite, CNT agglomerates are dragged along with the polymer matrix and pulled apart since the bonds between CNT agglomerates and the polymeric matrix are stronger than the bonds within the CNT agglomerate [33]. If there is no failure (permanent deformation, internal cracking, etc.), releasing the composite (unloading) restores contact between the CNT agglomerates. Since the electrical resistivity of the nanocomposite is affected by the distance between the conductive particles (i.e. CNTs), it can be used as a measure of strain, and indirectly, a composite health monitoring tool. Note that in fabrication of nanocomposite sensors, CNTs can be incorporated in different polymers such as poly (dimethylsiloxane) (PDMS) [34,35] and epoxy [31,32]. Although the fabricated sensors with CNT/PDMS are more flexible; CNT/epoxy are widely used in structural health monitoring of the laminated polymer composites.

Although the sensitivity of the electrical and mechanical properties of CNT/epoxy to resin-filler dispersion was investigated in several studies [24,25,36,37]; a reliable model that could show the effect of fabrication parameters and their interactions on the properties of nanocomposites is still lacking, and the effect of the dispersion process on the piezoresistive properties of the end composite has not been adequately investigated.

In this paper, the effect of dispersion and alignment of CNTs on electrical and electromechanical properties of CNT/epoxy nanocomposites is studied. Effect of shear mixing parameters (time and speed) on electrical conductivity and tensile strength of the epoxy/CNT samples at different CNT concentrations is investigated. Response Surface Methodology (RSM) is used to design the experiments and the results are analyzed statistically to understand the most influential process parameters and their interactions. For this purpose, over 100 samples are fabricated for electric conductivity measurements and over 50 tensile tests are performed for the mechanical characterization of the nanocomposites. Optical microscopy is used to study the morphology of CNT fillers in the liquid epoxy matrix, where the dispersion state of CNT in the epoxy matrix is expressed through quantitative (rather than qualitative) indicators. The resulting electrical and mechanical properties of nanocomposite samples are discussed in relation to the corresponding macrostructure. In addition, the effect of the CNT dispersion state (within the liquid epoxy) on the piezoresistivity of the end composites is addressed through the results.

In order to study the effect of post dispersing of CNTs on electrical conductivity of nanocomposite, CNT/epoxy suspension is subjected in a magnetic field during curing process. A 2D percolation-based model is used to simulate the electrical conductivity and piezoresistivity of the nanocomposites by considering the alignment of CNTs.

Preparation and characterization of nanocomposite

Materials and samples preparation

Nanocomposite samples were manufactured consisting of electrically conductive nanoparticles in a polymeric matrix consisting of epoxy resin

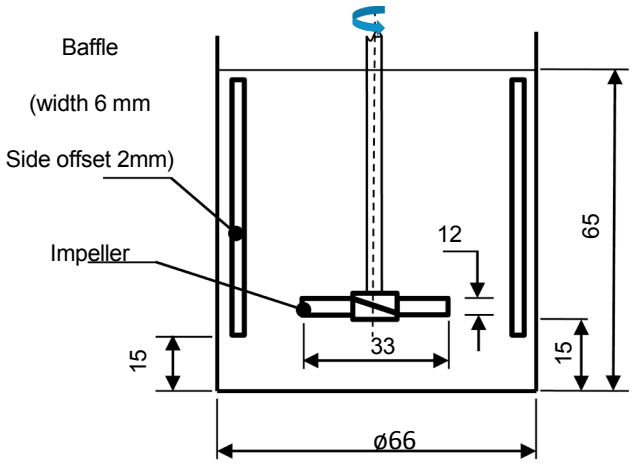

Fig. 1. Dimensions and layout of shear mixing setup. Dimensions are in mm.

(Araldite LY564, Huntsman) and hardener (Aradur 3486, Huntsman). Multi-Wall Carbon Nanotubes (MWCNTs), provided by Nanografi Co. Ltd. (Turkey), with an average diameter of 10 nm and average length of 1.5 μm (aspect ratio = 150) were used as the conductive nanoparticles. The CNT/epoxy suspensions were prepared by shear mixing of the components in a cylindrical vessel using a mechanical stirrer (MTOPS, MS3020D). A 3-blade turbine impeller with a pitch angle of 45° was used for shearing. Impeller blade numbers and blade geometry were selected to have an efficient axial flow pattern and minimum vortex, and to minimize the samples volume [38,39]. The vessel was equipped with four equally spaced flat wall baffles. Wall baffles provide top to bottom mixing by converting tangential flows to vertical flows which prevents swirling motion, minimizes vortexing and air entrainment [40]. Fig. 1 shows the geometrical configuration of the mixing equipment.

The vessel was filled with 150 gr of epoxy resin. Then the pre-weighted CNTs were added in several steps while stirrer was run at desired speed. At the end of the process, hardener was added with hardener-epoxy weight ratio 35:100. The suspension was further mixed for one minute at the same speed. Finally, in order to release trapped air the suspension was degassed under vacuum. Note that by adding more CNT the removal of the voids becomes more difficult due to high viscosity of the suspension and samples need to be more under vacuum. Here, degassing was done for 10 up to 30 min respectively, for low and high concentrated suspensions.

Design of experiments using response surface methodology

Response surface methodology (RSM) is a series of statistical and mathematical techniques used for modeling and analyzing the effect of known factors on a response with the objective of optimizing the response [41]. Using RSM, the response can be modeled as a second order polynomial of the form:

$$y = \beta_0 + \sum_{i=1}^{n} \beta_i x_i + \sum_{i=1}^{n} \beta_{ii} x_i^2 + \sum \sum_{i<j} \beta_{ij} x_i x_j + \epsilon \quad (1)$$

where x_i and x_j are the factors; β_0, β_i, β_{ij} and β_{ii} are the regression coefficients which are estimated using least squares method and ϵ characterizes the error observed in the response y.

The presented model (Eq. (1)) is a general model containing all predictor factors, their interactions and higher order (quadratic) terms. The significance of each term can be checked by running statistical tests (F test) and non-significant terms can then be eliminated from the model.

In this work, a series of experiments were designed using Response Surface Methodology (RSM) to study the effect of shear mixing parameters (mixing time and mixing speed) on the electrical conductivity and the tensile strength of the epoxy/CNT composite samples at various CNT filler

Table 1
Experimental factors and levels.

Factors	Levels		
	−1	0	1
CNT concentration (wt%)	0.2	0.35	0.5
Mixing speed (rpm)	500	1250	2000
Mixing time (min)	10	35	60

Table 2
RSM design matrix.

Run order	Mixing speed level	Mixing time level	CNT concentration level
1	−1	−1	−1
2	1	−1	−1
3	−1	1	−1
4	1	1	−1
5	−1	−1	1
6	1	−1	1
7	−1	1	1
8	1	1	1
9	−1	0	0
10	1	0	0
11	0	−1	0
12	0	1	0
13	0	0	−1
14	0	0	1
15	0	0	0
16	0	0	0
17	0	0	0
18	0	0	0
19	0	0	0
20	0	0	0

concentrations. The statistical software MINITAB 16 was used for the design of experiments as well as the statistical analysis of the results. The factors with their respective levels and the design matrix are presented in Tables 1 and 2, respectively. Based on the design matrix, 20 samples were manufactured for analysis and characterization.

Morphological study of CNT/epoxy suspensions

The quality of the dispersion process was studied through the morphology of the prepared suspension samples. 1 cc samples were taken out from the epoxy/CNT suspensions at specified time instances during the mixing operation. The samples were laid upon glass laminates and images were captured from each sample through optical microscopy at a magnification of 400. On each sample, 5 images at different locations of the sample were captured. The images were analyzed using the ImajeJ software [42] in which CNT clusters were distinguished from the matrix background by converting the captured imagery into binary format. The number of detected clusters for cluster areas greater than 20 μm^2, and the cluster areas in each image were determined. The results were used to analyze the dispersion state of CNT in epoxy, and correlate the dispersion conditions with the composite properties.

Post dispersing of CNTs via magnetization

In this study, the magnetic field approach was used to align CNTs. A magnetic field of 0.2 T was generated using a solenoid. Table 3 shows the chemical composition of CNT which was provided by supplier. It is worth to note that due to ferromagnetic properties of the residual catalysts such as Fe, Ni, or Co, used in fabricating CNTs, incompletely purified CNTs can respond well to low magnetic fields (typically 0.1–0.6 T) and are hence aligned in the polymer matrix [26,29].

A CNT/epoxy suspension was prepared by dispersing 0.5 wt% CNT into an epoxy matrix using shear mixing. The suspension was then

Table 3
Element composition of CNT.

C (at%)	O (at%)	Fe (at%)	Co (at%)	Cu (at%)	Zn (at%)
> 90	3.01	1.27	< 0,50	3.51	1.72

mixed at 2000 rpm for 1 h. Finally, 50 cc of the prepared suspension was subjected into vacuum for 10 min to remove the voids.

Three samples were prepared by injecting CNT/epoxy suspension into plastic tubes of diameter 2 mm and length 80 mm. Two of the samples were placed into a solenoid as a core. The solenoid was powered with 25 VDC at 2A and samples were kept under the magnetic field for 4 h. Here, the magnetized samples are labeled as MS1 and MS2, and NMS denotes not magnetized sample.

Characterization of CNT/epoxy nanocomposites

Measurement of electrical conductivity of CNT/epoxy nanocomposites

Nanocomposite samples were prepared by casting the prepared CNT/epoxy suspensions into thin, rectangular aluminum molds (dimensions 55 mm × 10 mm × 5 mm). The molds were placed in the oven following casting and cured at 80 °C for 8 h. After curing, samples were de-molded, and the long ends were trimmed, polished using Sic sand paper and washed with acetone for smooth end sections. The end sections were then painted with silver and let dry at room temperature.

The electric resistance of the samples along their length was measured using Two Point Probe Technique [43] with a Keithley 2000 Digital Multimeter. Fig. 2 presents the aluminum mold, specimens and the electrical resistance measurement configuration in which the probes are brought into contact with the silver-coated ends. The dimensions of the composite samples were measured using a digital caliper. Electrical conductivity is calculated using the measured parameters in Eq. (2) as

$$\sigma = \frac{L}{R \times A} \tag{2}$$

where σ is the electric conductivity, L is the sample length, R is the DC resistance (ohms) and A is the cross section area of the sample.

Mechanical characterization of CNT/epoxy nanocomposites

Uniaxial tensile tests were performed to study the electrical response of the prepared nanocomposites to strain. The tensile strength of the specimens was also recorded during the tests. Dog-bone shaped test specimens with a gauge length of 50 mm, a width of 13 mm and a thickness of 5 mm were prepared by casting CNT/epoxy suspensions into aluminum molds. Samples were cured at 80 °C for 8 h. After demolding, the ends of the samples were trimmed, polished, washed and painted with silver. Two copper wires (connected to the multimeter probes) were attached to the silver-coated ends using aluminum tape. Tensile tests were run according to ASTM D638 under displacement control by straining at a rate of 0.5 mm/min using a universal tensile test machine (Tenson). Wood stickers were used to create an electrical isolation barrier between the metal grips of the tensile machine and the conductive samples. To measure the strain, an extensometer with a gauge length of 50 mm was used. The force-elongation and electric resistance data were monitored and recorded using Labview software (National Instruments). The experimental set up and the test specimen are shown in Fig. 3.

Characterization of magnetized CNT composites

The morphologies of the fracture surfaces of the CNT/epoxy samples were examined using scanning electron microscopy (SEM). The samples for morphology inspection were prepared by cutting a small segment of maximum length 2 mm from a master sample (Fig. 4, sec A-A). These

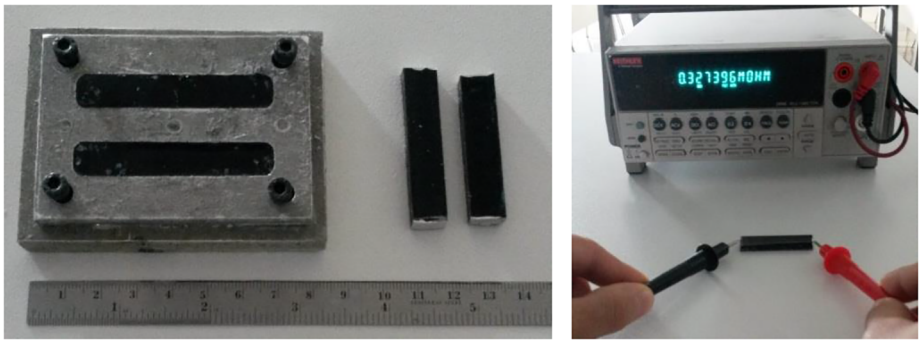

Fig. 2. Preparation of nanocomposite samples for electric conductivity measurement, (a) mold and specimens with silver-coated ends, (b) electrical resistance measurement.

small pieces were then split into two (Fig. 4, sec B-B).

Modeling of the electrical and electromechanical behavior of CNT/epoxy nanocomposites

A 2D resistor network model was used to investigate the electrical and electromechanical properties of CNT-filled nanocomposites. In a resistor network model, each CNT is considered as a resistor. Therefore, a CNT-filled nanocomposite above the percolation threshold can be modeled as a network of resistors that form conductive paths between two surfaces, or source and drain electrodes. This concept is shown in Fig. 5.

Here, CNTs were simulated as straight lines of length L_{CNT} and were distributed on a representative 2D area of length L and width W. Each nanotube was located by determining its two endpoints in a Cartesian coordinate system whose origin was fixed at the left-bottom corner of the representative area. The first endpoint location (x_1, y_1) was determined randomly, with x_1 and y_1 random numbers in [0, L] and [0, W], respectively. The other endpoint position, (x_2, y_2), was then calculated using the following equations:

$$x_2 = x_1 + L_{cnt}\cos\theta, \quad -\frac{\pi}{2} \le \theta \le \frac{\pi}{2} \tag{3}$$

$$y_2 = y_1 + L_{cnt}\sin\theta, \quad -\frac{\pi}{2} \le \theta \le \frac{\pi}{2} \tag{4}$$

where θ is the nanotube's orientation angle.

Upon generating CNTs with a concentration N, the locations of intersecting points (junctions) were identified by solving sets of linear equations. Then, graph theory was used to find the available paths between any two points, or between source (S) and drain (D) electrodes. As illustrated in Fig. 6, the graph model assumes that each CNT includes a graph vertex and the junction between nanotubes is an edge between two corresponding vertices.

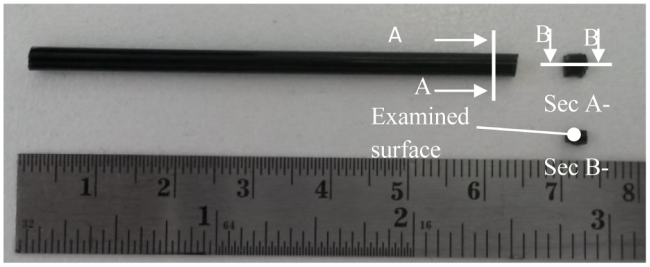

Fig. 4. Preparing a fractured surface for SEM characterization.

In Fig. 6, the parameter of interest is the total electrical resistance between source and drain electrodes. The resistance of segments between junctions can be calculated as [44]:

$$R = R_t\left(1 + \frac{l_c}{\lambda}\right) + R_{jct} \tag{5}$$

where R_t is the theoretical contact resistance at the ballistic limit with an approximate value of 6.5 kΩ and 100 kΩ for SWCNT and MWCNT

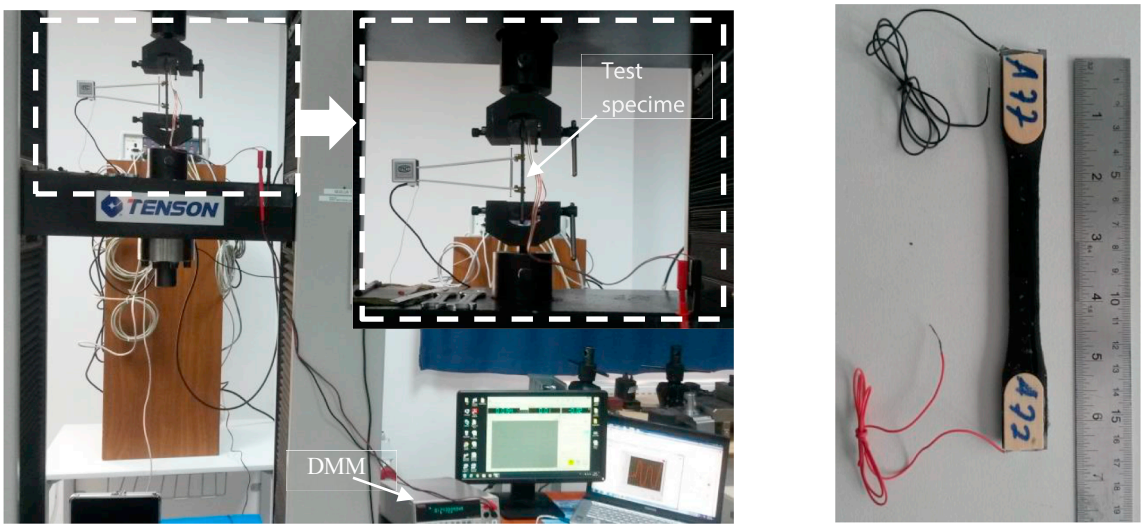

(a) (b)

Fig. 3. (a) Tensile test set-up for studying the electrical resistance of CNT/epoxy nanocomposites under loading, (b) Composite test specimen.

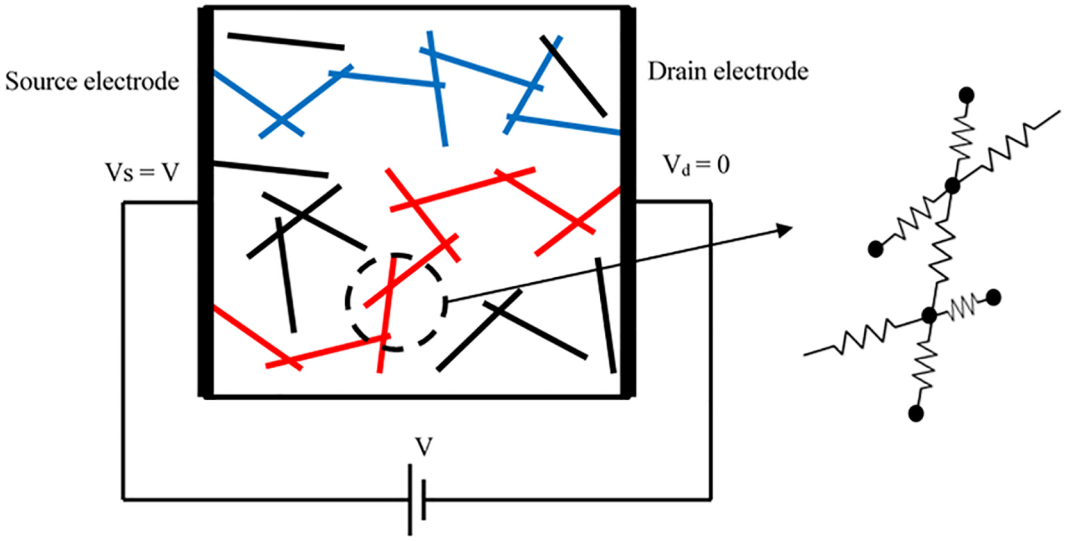

Fig. 5. Schematic of resistor network model.

respectively, λ is the electron mean free path (assumed to be 1 μm), l_c is the length of the conductor (nanotube segment between neighboring junctions), and R_{jct} is the nanotube-nanotube junction contact resistance. Fig. 7 shows the modeling of nanotube resistance using equivalent resistors.

Finally, network resistance can be calculated using nodal analysis, i.e., Kirchhoff's current law, [44–46] or graph conductance theory [47].

In this study, the entire network resistance was calculated using graph conductance theory. First, the resistance of all available paths along the length of the representative element (L) was calculated. In other words, the nanotube network was considered as a circuit consisting of several connected resistors (in parallel or series) that form conductive paths between the source and drain electrodes. Then, the network overall resistance can be calculated using Ohm's law. In this study, the simulation code was implemented in MATLAB (Mathworks, Inc.).

In CNT nanocomposites, carbon nanotubes are significantly stiffer than the polymer matrix material. For instance, the elastic modulus of a typical epoxy resin is around 3 GPa, nearly 300 times less than that of CNTs [48]. Thus, when nanocomposites are subjected to tensile or compression strain, the amount of strain at the nanotubes can be neglected compared to the matrix strain [47]. Therefore, when the matrix is deformed, nanotubes are just displaced from their initial positions in the matrix, and consequently, the conductive network reconfigures itself and the nanocomposite resistance changes. To be specific, if a strain ε is applied to a representative area along y axis, the new location and orientation of nanotubes can be updated using following equations:

$$x_1' = x_1(1 - \varepsilon\vartheta) \tag{6}$$

$$y_1' = y_1(1 + \varepsilon) \tag{7}$$

$$\theta' = \tan^{-1}\left[\frac{1+\varepsilon}{1-\vartheta\varepsilon}\tan(\theta)\right] \tag{8}$$

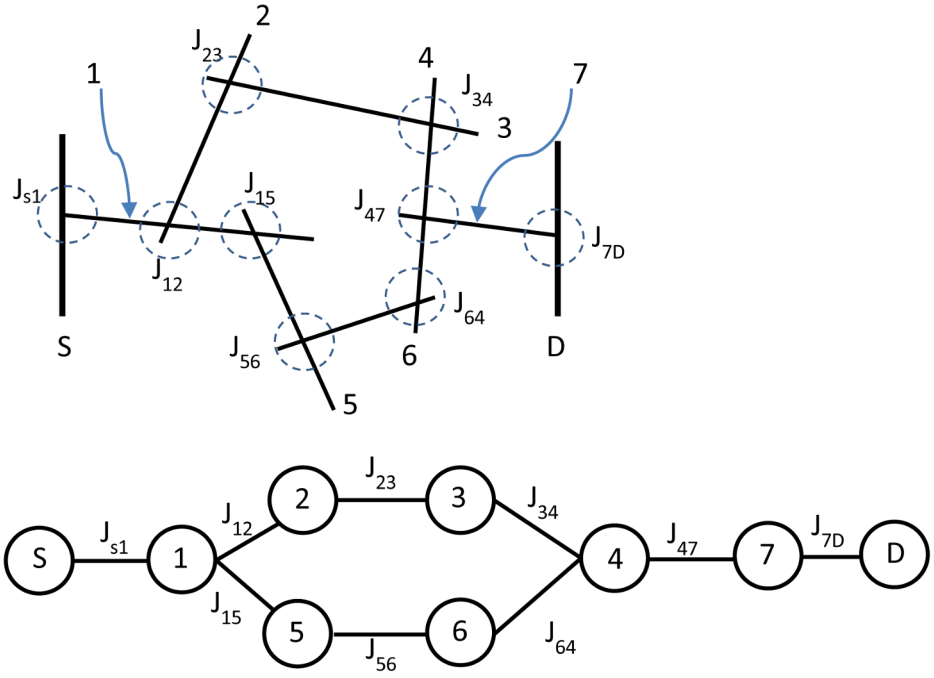

Fig. 6. Equivalent graph of a nanotube network, (a) randomly distributed nanotube network between source (S) and drain (D) electrodes, (b) equivalent graph for resistance analysis of nanotube network.

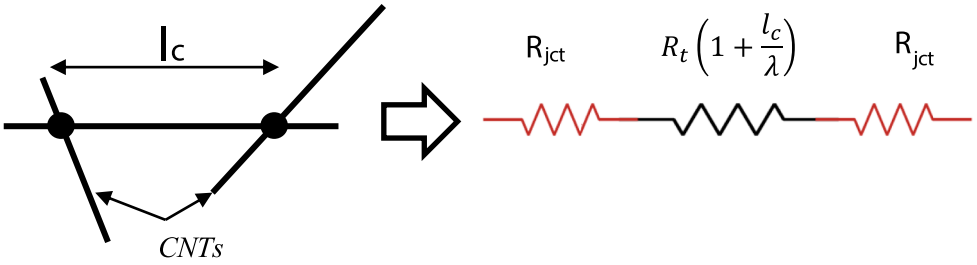

Fig. 7. Equivalent resistance of a nanotube segment between two junctions.

where x_1', y_1', and θ' are the updated coordinates and direction of nanotubes and ϑ is the Poisson ratio of the matrix (here, $\vartheta = 0.35$).

Upon doing so, the electrical resistance of reconfigured CNT network is then calculated using the same procedure outlined at the beginning of this section. Finally, strain sensitivity (k) or strain gauge factor is calculated as:

$$k = \frac{(\Delta R/R_0)}{\varepsilon} \tag{9}$$

where R_0 is the initial resistance when unstrained, and ΔR is the change in electrical resistance of the nanocomposite for strained and unstrained cases.

Results and discussion

Dispersion state of CNTs in epoxy matrix

Fig. 8 shows the CNT clusters (darker areas) in epoxy matrix. The experiment labels state suspension mixing conditions. For instance, 500N10T20W denotes the sample mixed at 500 rpm for 10 min, with 0.2 wt% of CNT. The results of CNT clusters distribution analysis based on clusters surface area are represented in Table 4. The dispersion state of CNT clusters was represented by citing A_{50}, A_{90} and A_{occ}. A_{50} and A_{90} are extracted respect to the cumulative area distribution of CNT clusters and indicate that the 50 and 90 percent of the detected CNT clusters have an area equal or less than these values, respectively. A_{occ} indicates the fractional area occupied by CNT clusters.

Considering Table 4, the occupied surface by CNT clusters (A_{occ}) were

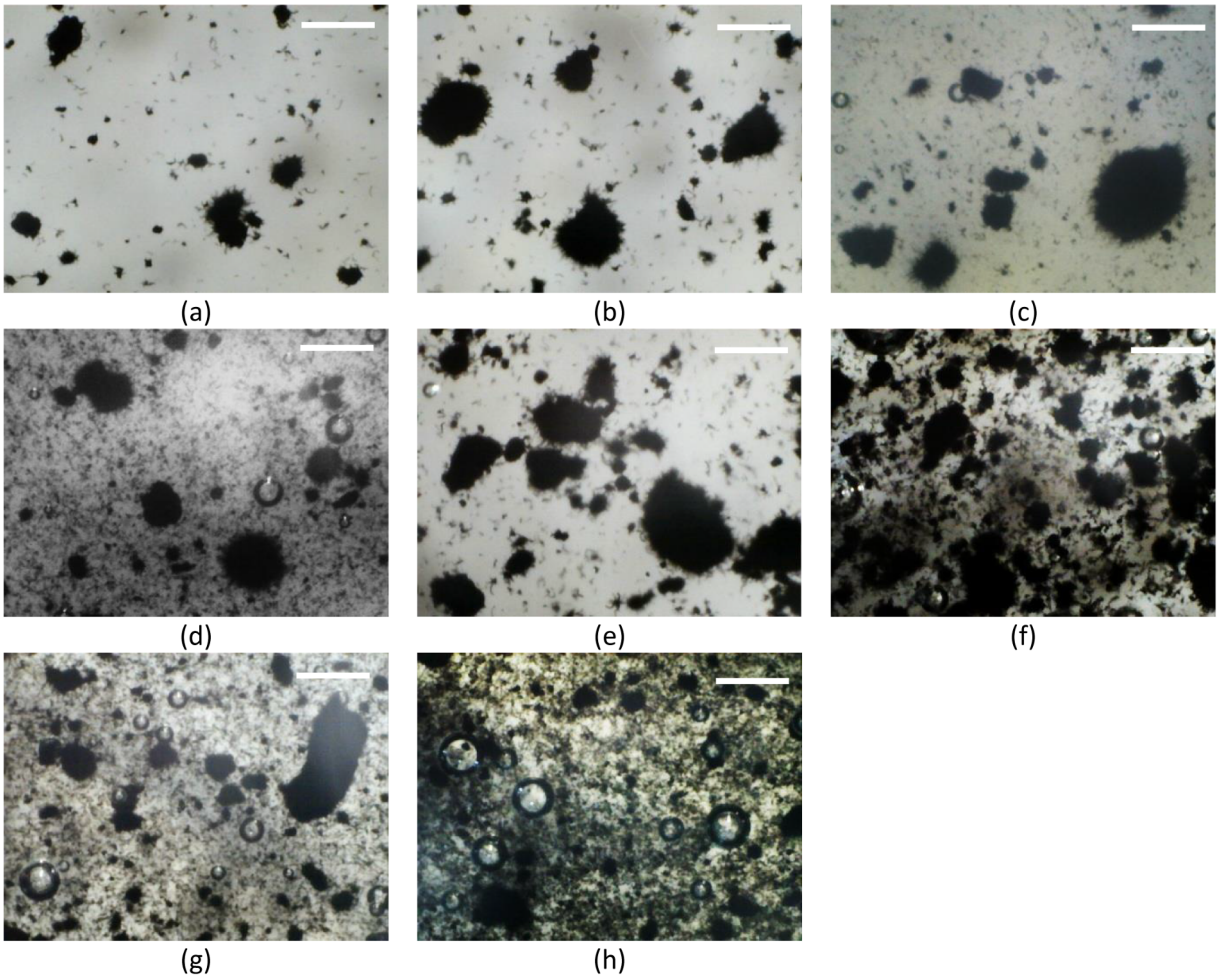

Fig. 8. Microscopy imagery of CNT/epoxy suspensions (a) 500N10T20W, (b) 500N60T20W, (c) 2000N10T20W, (d) 2000N60T20W, (e) 500N10T50W, (f) 500N60T50W, (g) 2000N10T50W, (h) 2000N60T50W, Scale bar is 200 μm.

Table 4
CNT clusters surface area distribution analyzes.

sample	Median area (A_{50}) – (μm^2)	A_{90} (μm^2)	Occupied area (Aocc) – (%)
500N10T20W	150	1600	8.4
2000N10T20W	90	700	16.3
500N60T20W	200	3000	17.1
2000N60T20W	70	500	18.6
500N10T50W	200	4000	26.1
2000N10T50W	90	1600	41.4
500N60T50W	200	3500	43
2000N60T50W	75	800	40.3
500N35T35W	150	2500	21
2000N35T35W	80	800	22.8
1250N10T35W	100	1200	22.9
1250N60T35W	100	2000	25.9
1250N35T20W	120	1500	14.3
1250N35T50W	120	1500	49.8
1250N35T35W	120	1300	24.5

Table 5
Tensile strength and electric conductivity of CNT/epoxy nanocomposites prepared with different mixing conditions and CNT concentrations.

Run order	Sample	Tensile strength (MPa)	Electric conductivity (S/m) × 10^{-3}
1	500N10T20W	55	0.198
2	2000N10T20W	81	0.102
3	500N60T20W	61	0.250
4	2000N60T20W	78	0.278
5	500N10T50W	58	4.230
6	2000N10T50W	74	4.950
7	500N60T50W	52	3.340
8	2000N60T50W	84	26.300
9	500N35T35W	52	1.660
10	2000N35T35W	84	2.310
11	1250N10T35W	63	1.200
12	1250N60T35W	75	2.240
13	1250N35T20W	71	0.185
14	1250N35T50W	66	5.980
15	1250N35T35W	76	1.460
16	1250N35T35W	72	2.140
17	1250N35T35W	79	2.500
18	1250N35T35W	72	2.300
19	1250N35T35W	80	2.680
20	1250N35T35W	75	2.420

measured less than 20% and more than 40% (except 500N10T50W) for samples involved 0.2 and 0.5 CNT wt%, respectively. Although sample 500N10T50W contains 0.5 CNT wt%, the surface area occupied by CNT clusters is 26.1%. The existence of large (A_{90} = 4000 μm^2) and dense (A_{occ} = 26.1%) clusters implies that applying low mixing speed with low mixing time was not sufficient to disperse CNTs in epoxy matrix, effectively. Fig. 8e shows the microscopic image of this sample where several large clusters can be seen in epoxy matrix. Also, a finer microstructure (A_{50} < 90 μm^2) can be obtained using higher mixing speed (2000 rpm) (Fig. 8d, g and h). The interaction effect of mixing time and CNT concentration on dispersion state can be noticed by considering the results obtained for samples which were mixed at 2000 rpm. Both 2000N10T50W and 2000N60T50W samples (at which 0.5 wt% CNT was mixed at 2000 rpm for 10 and 60 min, respectively), although; the occupied area by the clusters (A_{occ}) and the observed clusters median area (A_{50}) are very close to each other; there is a noticeable difference in their respective A_{90} values. Using higher mixing speeds for longer periods of time is effective to obtain a finer macrostructure at higher CNT concentrations. However, the obtained morphology is similar for the low CNT-concentration samples that are mixed at 2000 rpm (2000N10T20W and 2000N60T20W) regardless of mixing time.

Electric conductivity and tensile strength of CNT/epoxy nanocomposites

Three samples were prepared under same experimental conditions according to the design matrix (Table 2). The averages of calculated electric conductivity based on Eq. (2) and measured tensile strength for each sample set, are shown in Table 5. Fig. 9 presents the measured conductivity for the samples in which mixing speed, mixing duration and CNT concentration were set to their low and high levels. From Fig. 9, it is seen that mixing parameters (speed and duration) and their interactions do not show considerable effect on electric conductivity when CNT concentration is at its lowest level (0.2 wt%). However, maximum conductivity (3.340 × 10^{-3} (s/m)) was measured for the case where mixing was performed with the lower mixing speed (500 rpm) for 60 min. This implies that, low mixing speed can provide sufficient shear force for dispersing CNTs in low concentrated CNT/epoxy suspensions with less care about over dispersing [24]. At higher CNT concentrations, the electric conductivity of the samples mixed at 2000 rpm for 60 min is nearly six times that of other samples with the same CNT concentration. At high CNT concentration where viscosity of epoxy/CNT suspension is high and there are significant aggregates of CNTs, low mixing speeds cannot create sufficient shear force to break down CNT agglomerates and disperse CNTs in epoxy matrix effectively

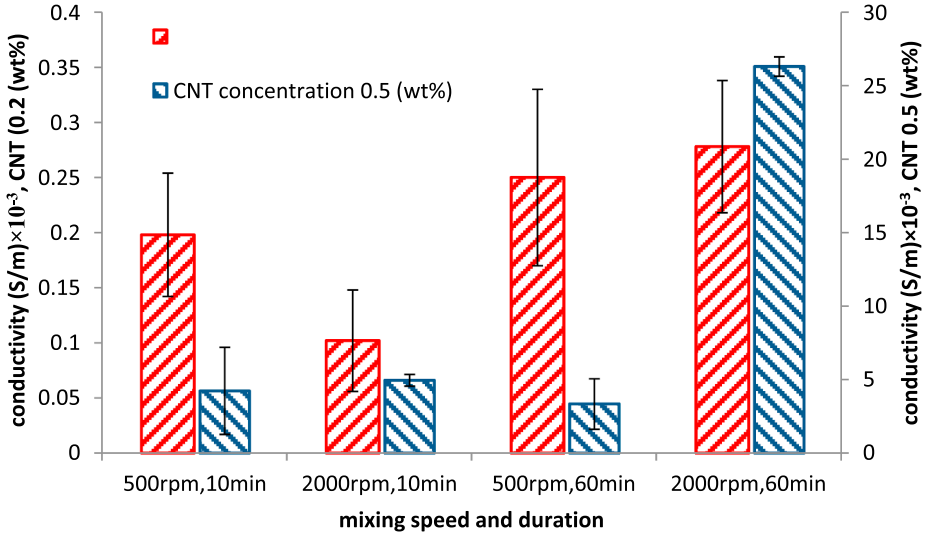

Fig. 9. Effect of mixing conditions and CNT concentrations on electric conductivity.

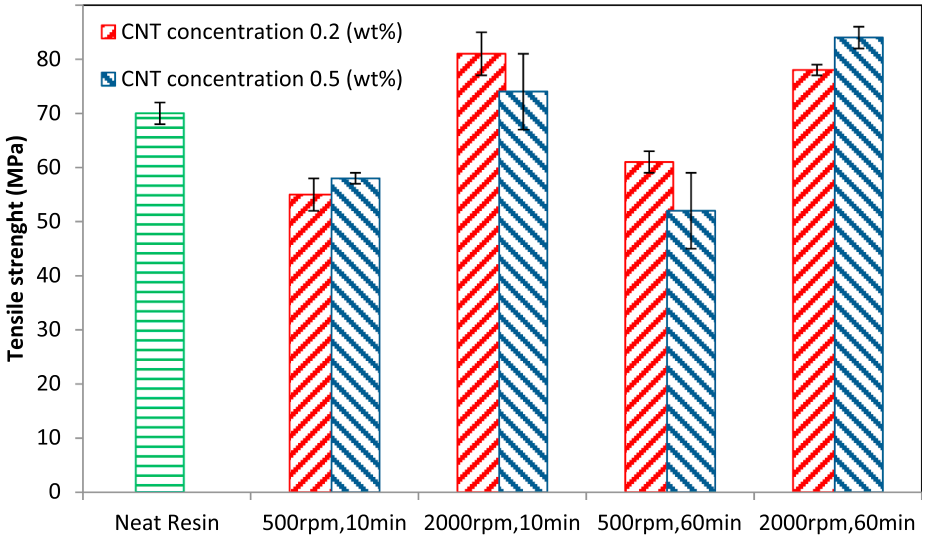

Fig. 10. Tensile strength of CNT/epoxy composites prepared at different mixing conditions and varying amounts of CNT.

(Fig. 8e–f).

Tensile strength of CNT/epoxy composites with varying CNT concentrations are presented in Fig. 10. The maximum tensile strength (84 MPa) was measured for the sample at which 0.5 wt% CNT was dispersed in epoxy matrix at 2000 rpm for 60 min (84 MPa). The minimum strength (52 MPa) was observed at sample prepared by mixing 0.5 wt% CNT at 500 rpm for 60 min. Tensile strength of all samples prepared with low shear force (500 rpm), regardless of mixing time and CNT concentration, alter between 52 up to 61 MPa and indicate a decreasing in strength comparing to not reinforced epoxy resin.

Fig. 11 presents the SEM images of the fracture surfaces of tested nanocomposites. Here, the A considerable different fractographic features are considerably varying. A smoother fracture surface with large CNT clusters is seen for the samples in which the mixing speed of suspension was low in Fig. 11a and d. Smaller CNT clusters and higher fracture surface roughness (Fig. 11g and j) were obtained for samples where high mixing speed was used to prepare the suspension. Analyzing the CNT clusters on fractured surface with higher magnifications shows that a more uniform microstructure can be obtained using higher mixing speeds (Fig. 11i and l). This result concurs with the obtained results through morphology study of CNT/epoxy suspension (Fig. 8c and h). Considering tensile test results and SEM results, it is seen that CNT/epoxy nanocomposites that have the higher strengths have finer structures (Fig. 11j–l). Such a structure obtains by mixing the suspension with high shear speeds and for longer durations (Fig. 8h). Conversely, existence of large CNT agglomerates, caused by dispersing CNTs at low mixing speeds and short times (Fig. 8f and Fig. 11d–f), resulted in forming stress concentration zones [9,49] which affects the strength of CNT/epoxy composite negatively. Similarly, it can be said that for any suspension mixing condition, there is an optimum CNT content above which the strength of nanocomposite is affected adversely due to ineffective dispersion process and existence macro-scale agglomerated CNT particles. These results confirm the effect of CNT dispersion state on mechanical properties of nanocomposites [10,15].

Analysis of variance (ANOVA) and regression models

In this paper, a systematic approach was used to obtain a reliable mathematical relation to present the effect of suspension preparation parameters and CNT content on electric conductivity and tensile strength of CNT/epoxy nanocomposites. These models can then be used to optimize preparation parameters and CNT contents to achieve the desired electrical and/or mechanical properties. Based on RSM (Eq. (1)), such a model can be presented as:

$$y = \beta_0 + \beta_1 N + \beta_2 T + \beta_3 W + \beta_4 N^2 + \beta_5 T^2 + \beta_6 W^2 + \beta_7 N.\ T + \beta_8 N.\ W + \beta_9 T.\ W \quad (10)$$

where y is electric conductivity or tensile strength, N is the CNT/epoxy suspension mixing speed in rpm, T is the CNT/epoxy suspension mixing time in minutes, W is CNT concentration in wt% and β_1-β_9 are unknown coefficients which are estimated using least squares method. Eq. (10) presents the effect of main factors (N, T and W), quadratic terms (N^2, T^2 and W^2) and their interactions ($N.T$, $N.W$ and $T.W$) on electric conductivity and tensile strength of nanocomposite.

Finally, ANOVA was used to determine the effectiveness of the process parameters on properties of nanocomposite. The details of ANOVA methodology are presented in Appendix.

The regression model of electric conductivity (10^{-3} × S/m) that fits the experimental data based on the results can be represented as:

$$\sigma = \exp(-5.341 - 0.001N - 0.009T + 26.65W - 26.85W^2 + (0.309 \times 10^{-2})N.\ T + (0.003)N.\ W) \quad (11)$$

where N is the CNT/epoxy suspension mixing speed in rpm, T is the CNT/epoxy suspension mixing time in minutes and W is CNT concentration in wt%.

A similar analysis has been employed for the effect of production parameters on CNT/epoxy nanocomposite strength and the results are given in Appendix. Considering the calculated P-values, mixing speed has the greatest effect on tensile strength of the samples. On the other hand, mixing duration does not show a significant effect on tensile strength.

Ultimate tensile strength (UTS, MPa) of CNT/epoxy can be represented using a regression model as follow:

$$UTS = -216.3 + 26.59N + 0.02T + 0.08W - 141.85W^2 \quad (12)$$

Validation of the mathematical models of conductivity and composite strength

To investigate the accuracy and robustness of the found regression models for conductivity and composite strength, 8 further experiments were carried out within the range of explored experimental parameters. Each “experiment” is the production of a new nanocomposite sample that has different production parameters (mixing conditions for preparation of the CNT/epoxy suspensions that are later cast and cured). These samples

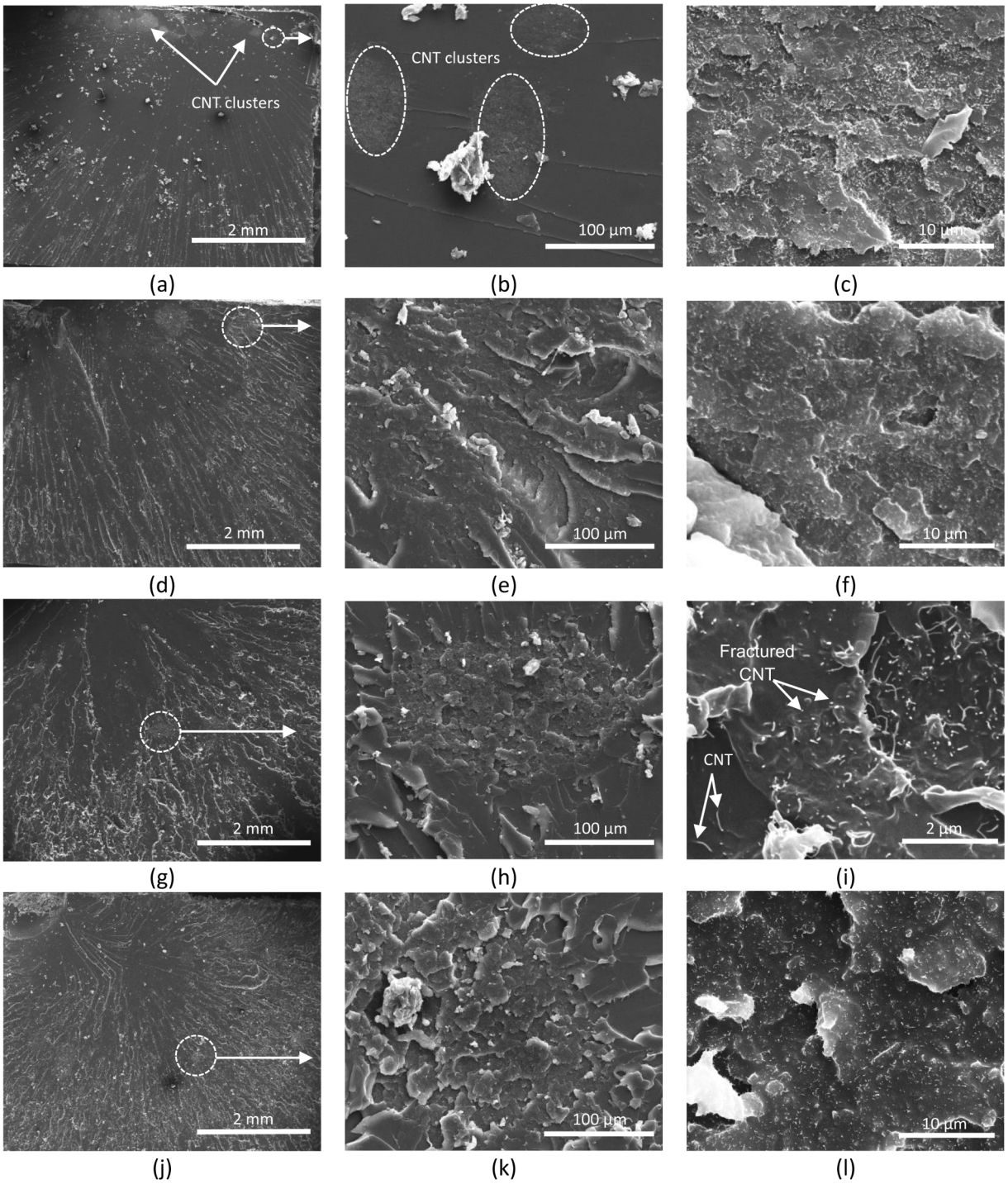

Fig. 11. SEM images of CNT/epoxy nanocomposite fracture surface, (a–c) 500N10T20W, (d–f) 500N60T50W, (g–i) 2000N10T20W, (j–l) 2000N60T50W.

were then tested for conductivity and tensile strength as outlined before. The results are compared with the predicted results from the regression models of Section "Analysis of variance (ANOVA) and regression models". Table 6 presents the predicted values and the experimental values (average of 3 samples) with the corresponding standard deviation. The tabulated results are shown in graphical form in Fig. 12. The estimated values are all within scattering range, indicating the developed regression models have acceptable robustness and accuracy within the range of explored experimental parameters (suspension mixing speed: 500 to 2000 rpm, suspension mixing duration: 10 to 60 min and CNT concentration: 0.2 to 0.5 wt%). The high residuals observed in some of the experiments based on which the regression models were developed in earlier analysis, did not prevent the acceptability of the developed models.

Strain sensing behavior of CNT/epoxy nanocomposites under tensile loads

Strain in a conductive nanocomposite during service can be related to the electrical conductivity of nanocomposite. The variation in electrical resistance can be used for measuring and monitoring the amount of strain in composite during service, if the conductivity of nanocomposite has sufficient sensitivity to strain. The sensitivity of a strain gauge to sense strain can be expressed quantitatively using

Table 6
Validation tests.

Exp. No.	Sample ID	Tensile strength (Mpa)			Electric conductivity (S/m) × 10^{-3}		
		Predicted	Experimental	2Std.	Predicted	Experimental	2Std.
1	800N10T30W	63.5	66	± 4	0.88	0.78	± 0.16
2	800N60T30W	67.2	70	± 8	1.14	1.29	± 0.52
3	1600N10T30W	76.4	80	± 6	0.68	0.648	± 0.30
4	1600N60T30W	80.2	78	± 6	1.79	1.57	± 0.60
5	800N10T40W	62.5	66	± 4	2.48	1.96	± 0.50
6	800N60T40W	66.3	71	± 8	3.21	2.76	± 0.52
7	1600N10T40W	75.4	79	± 4	2.43	2.33	± 0.64
8	1600N60T40W	79.3	76	± 6	6.42	5.87	± 0.78

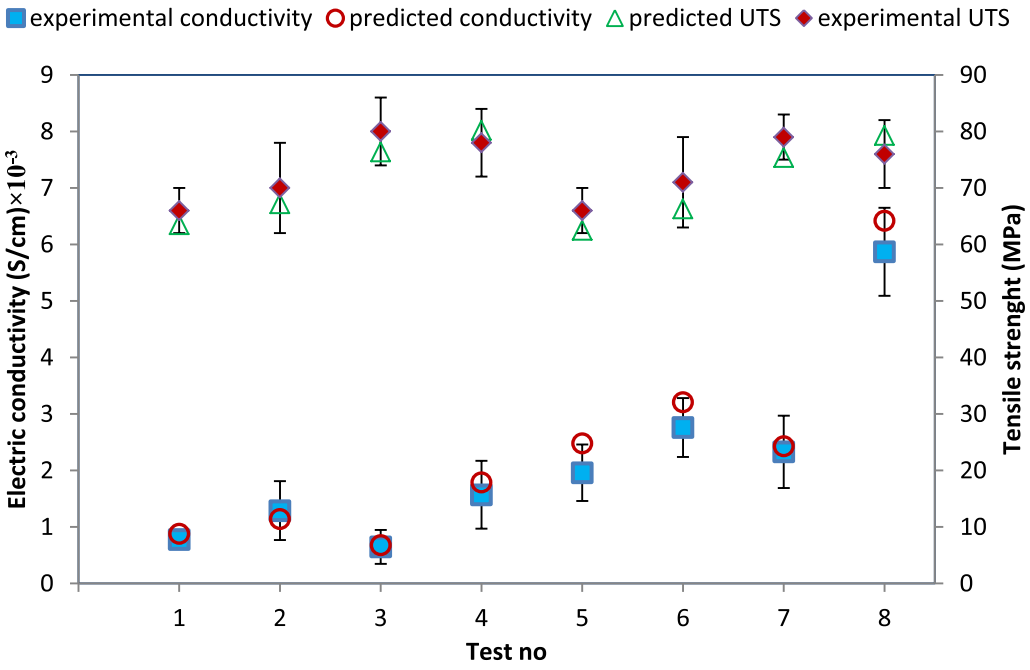

Fig. 12. Estimated and experimental Electric conductivity of samples presented in Table 6.

$$k = \frac{\Delta R/R_0}{\varepsilon} \tag{13}$$

where k is gauge factor, $\Delta R/R_0$ is the change of the electrical resistance ΔR normalized by the initial resistance R_0 and ε is strain [50]. The fractional change in electrical resistance ($\Delta R/R_0$) versus the strain during the testing of the samples is presented in Fig. 13a and b. Gauge factor is obtained by curve-fitting a straight line to the experimental data of Fig. 13.

Bias and nonlinearity are used to determine the accuracy of (nanocomposite) sensors in sensing the strain. The % bias value is given as:

$$Bias = \left(\frac{1}{n}\sum_{i=1}^{n}\frac{|\varepsilon_i - \hat{\varepsilon}|}{\varepsilon_{max}}\right) \times 100\% \tag{14}$$

and indicates how much gauge bias explains the overall process variation [51]. Here, ε_i is the measured strain, $\hat{\varepsilon}$ is the predicted strain (based on composite electrical resistance) and ε_{max} is the maximum measured strain.

Deviation from linearity is calculated using

$$Nonlinearity = \frac{|k\varepsilon - \Delta R/R_0|}{\varepsilon} \times 100\% \tag{15}$$

and describes how accurate the measurements are through the expected range of measurements [50]. The effect of CNT filler concentration and dispersing scenario on sensory properties of the CNT/epoxy nanocomposites is presented in Table 7.

Regardless of mixing factors, gauge factor of nanocomposites with low CNT concentration (0.2 wt%) varies between 1.5 and 2.9 which is too wide comparing to scattering in k-factor of the high CNT loaded composites (1.3 up to 1.6). This can be observed in Fig. 13 where for low concentrated samples; a significant difference between the responses of the composite sensors ($\Delta R/R_0$) under tensile strain can be observed (Fig. 13a). On the other hand, the fractional change in electrical resistance ($\Delta R/R_0$) of the samples containing high amount of CNT under axial tensile strain is significantly close to each other. Considering above discussion, it can be say that sensitivity (k-factor) of high CNT concentrated is not affected by mixing scenario in contrast to low concentrated nanocomposites where other sensory properties (bias, nonlinearity) are also affected by mixing parameters. According to Table 7, considering bias less than 10%, the maximum sensitivity (k = 2.9) was observed for the sample at which 0.2 wt% CNT was dispersed in epoxy matrix at 2000 rpm for 60 min. It implies that finer morphologies are more sensitive to strain and are more suitable for strain sensing applications.

Fracture surface analysis of magnetized nanocomposites

The SEM images of the samples prepared with and without an applied magnetic field (Fig. 14) differ based on the geometry of the detected CNTs. Most of the detected CNTs on the fractured surface of the samples that were not subjected to a magnetic field are in the form of a circle. On the other hand, by applying a magnetic field, the CNTs lay on the fractured surface. This can be quantified by counting the observed

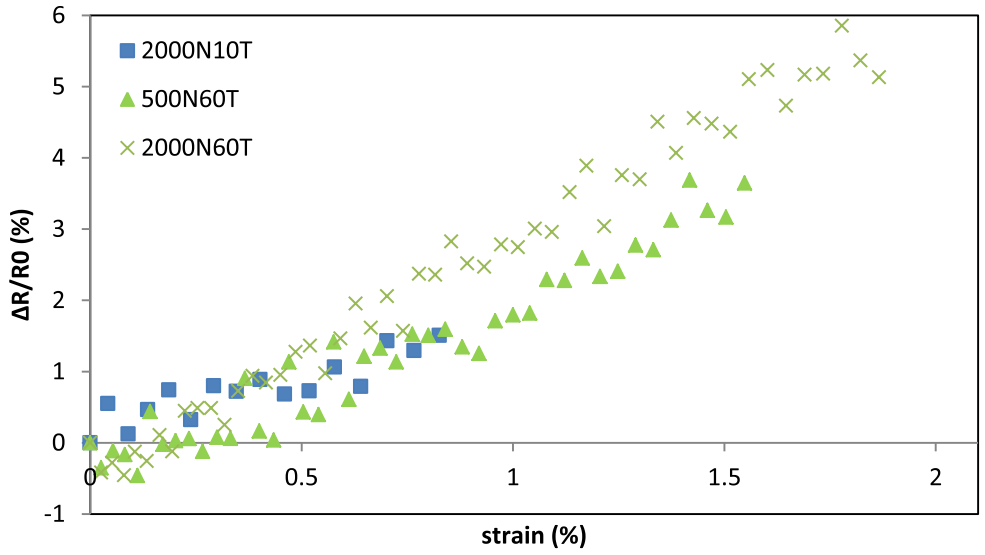

(a)

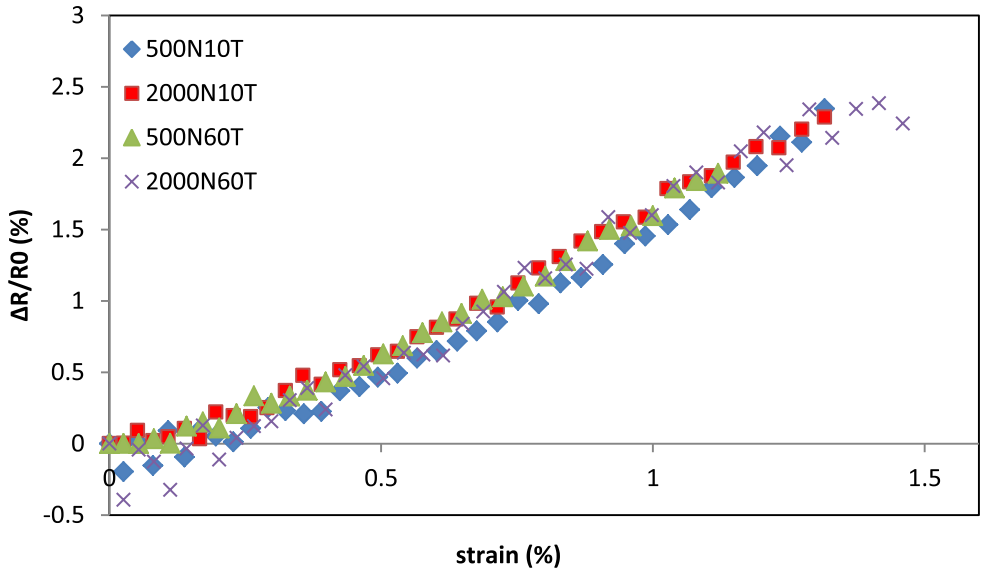

(b)

Fig. 13. The fractional change in electrical resistance ($\Delta R/R_0$) verses strain of the samples containing (a) 0.2 and (b) 0.5 wt% CNTs.

Table 7
Effect of mixing parameters and CNT concentration on sensory properties of CNT/epoxy nanocomposites.

Mixing speed (rpm)	Mixing time (min)	CNT concentration (wt%)	Gauge factor (k)	Bias max	Bias (%)	Nonlinearity (%)
500	10	0.2	–	–	–	–
2000	10	0.2	1.8	32.2	11.8	20.4
500	60	0.2	2.0	28.1	10.6	24.7
2000	60	0.2	2.9	12.1	5.4	13.0
500	10	0.5	1.4	22.8	10.1	26.2
2000	10	0.5	1.6	11.0	5.7	14.0
500	60	0.5	1.5	9.7	6.6	16.5
2000	60	0.5	1.5	19.1	7.5	18.5

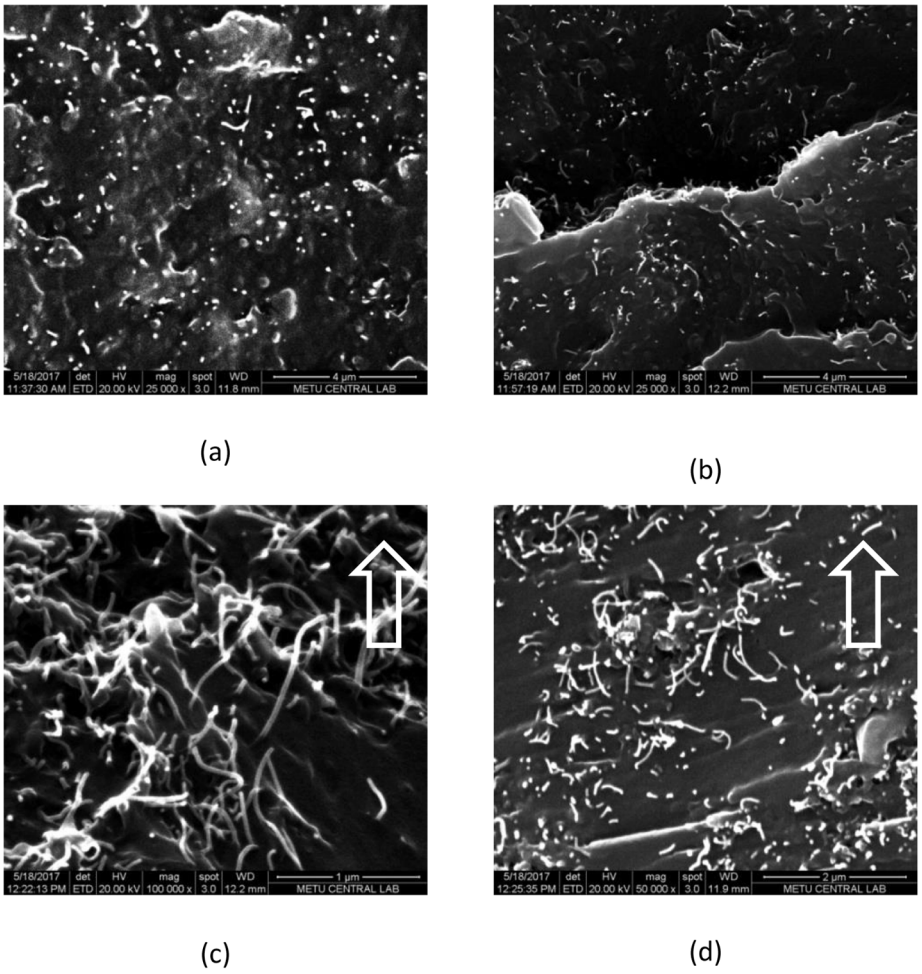

Fig. 14. SEM micrographs of fracture surfaces of CNT epoxy containing 0.5 wt% CNT. (a) Not magnetized. Sapmle, NMS, (b–c) Magnetized samples, MS1 and MS2. Surfaces are parallel to magnetic field. Arrows show the direction of magnetic field.

circles. According to ISO 9276-6, circularity is defined as the degree to which the object is similar to a circle, taking into consideration the particle form and roughness. Circularity is a dimensionless value and calculated using following equation:

$$C = \sqrt{\frac{4\pi A}{P^2}} \tag{16}$$

where C is the circularity, A is the area, and P is the perimeter of the object.

Analysis of the SEM images (Fig. 14) using ImageJ shows that the ratio of detected CNTs with circularity greater than 0.7 to the number of total detected CNTs for the samples subjected to a magnetic field varied between 0.21 and 0.30. The same ratio for nanocomposite samples not subjected to a magnetic field was in the range 0.55–0.68.

Histogram of CNT orientation angles of the composites were plotted in MATLAB® using processed SEM micrographs from ImageJ. These histograms (Fig. 15) were used to investigate the effect of magnetization on dispersion state of CNTs. Note that obtaining a perfect alignment was not expected using 0.3 T magnetic field due to the high viscosity of the CNT/epoxy suspension [29].

Effect of magnetization on electrical conductivity of CNT/epoxy nanocomposite

Six magnetized CNT/epoxy samples were fabricated by replicating the process described in Section “Post dispersing of CNTs via magnetization”. The samples were cut and polished at their ends and then painted using silver paint. The electrical resistance of the samples along their length was measured using a two-point-probe technique [43] with a Keithley 2000 Digital Multimeter. The electrical resistance of the samples was measured as 170 ± 30 kΩ, nearly half of the measured resistance of the control samples (380 ± 50 kΩ). Thus, a significant improvement in the electrical conductivity of the CNT/epoxy nanocomposite was obtained by applying a magnetic field.

Simulation results

Using the proposed percolation model, the effect of CNT alignment on percolation probability of nanocomposites was simulated. The percolation probability is calculated using Eq. (17):

$$P = \frac{N_c}{N_{ts}} \tag{17}$$

where N_{ts} is the total number of simulations, and N_c is the number of cases in which the model is electrically conductive. To calculation percolation probability, CNTs with length of 1.5 μm were distributed in a $7.5 \times 7.5\ \mu m^2$ area [44] with presented distribution functions at Fig. 15 and the simulation was conducted 100 times for each cases. A Monte Carlo simulation was used for this purpose. The simulation results are shown in Fig. 16. According to simulation results, nanocomposite with aligned nanotubes reaches to percolation threshold (50% percolation probability) at lower CNT concentrations than nanocomposites with random nanotubes.

Fig. 17 shows that, the electrical resistance of the percolated CNT

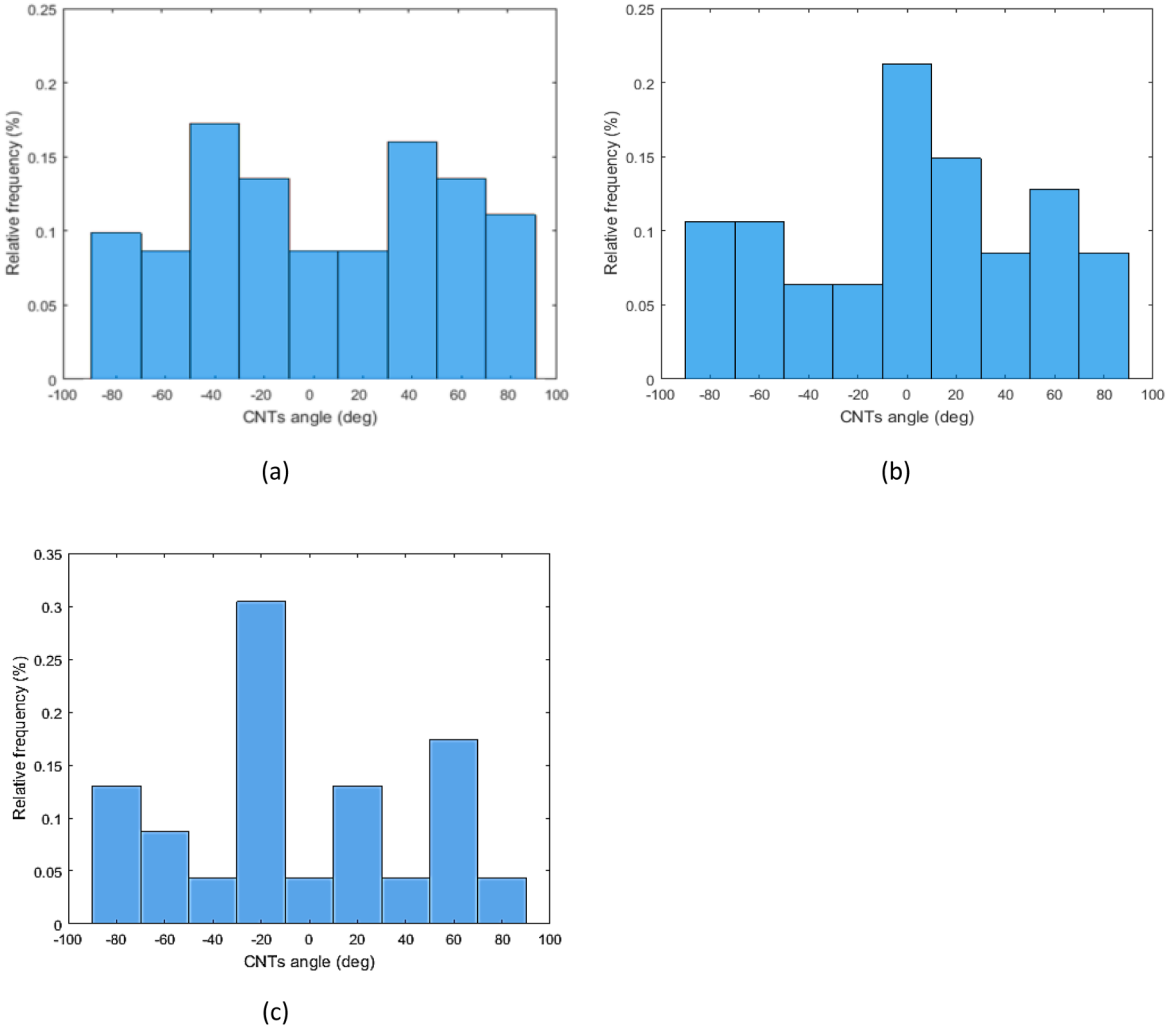

Fig. 15. Histograms of CNT orientation angles of CNTs in the composites (a) not subjected to the magnetic field, NMS, (b–c) subjected to the magnetic field, MS1 and MS2.

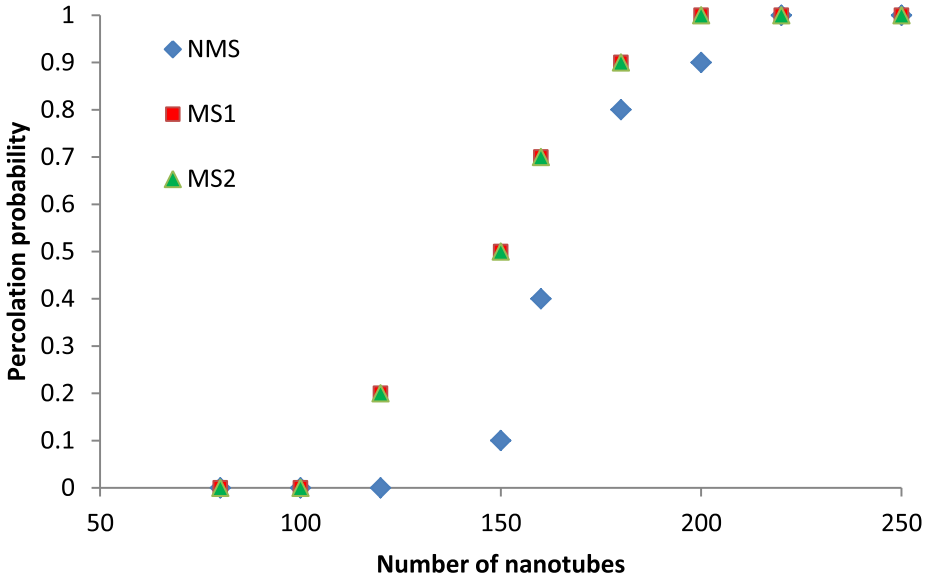

Fig. 16. Effect of nanotubes distribution on the calculated percolation characteristics of $7.5 \times 7.5\,\mu m^2$ CNT based nanocomposite models. $L_{CNT} = 1.5\,\mu m$, $R_t = 100\,k\Omega$, $R_{jct} = 1\,k\Omega$.

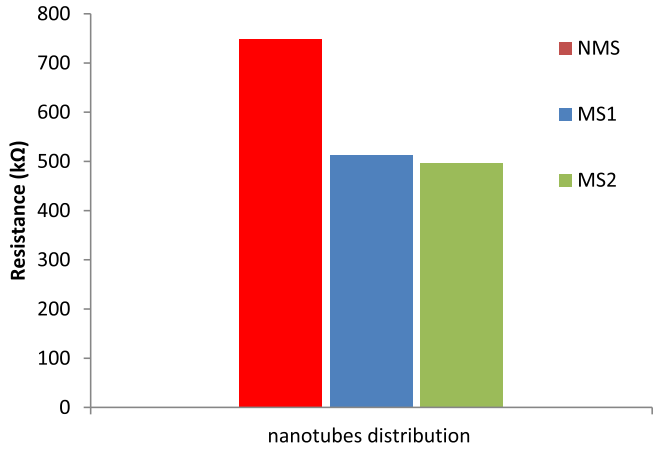

Fig. 17. Effect of nanotubes distribution on the calculated electrical resistance of $7.5 \times 7.5\,\mu m^2$ CNT based nanocomposite models. N = 250 and $L_{CNT} = 1.5\,\mu m$, $R_t = 100\,k\Omega$, $R_{jct} = 1\,k\Omega$.

networks (N = 250) with a random distribution is much higher than the networks consist of aligned CNTs. In case of random distribution, the resistance of simulated CNT network is 748 kΩ and for the cases in which CNTs were distributed according to the presented distribution patterns in Fig. 15b and c, the resistance of model is 512 kΩ and 497 kΩ, respectively. In another word, the simulation results show that the electrical conductivity of CNT networks with the same morphology as Fig. 15b and c is 1.5 times higher than the nanocomposite with random CNT distribution. This finding is in good agreement with the presented experimental results in Section "Effect of magnetization on electrical conductivity of CNT/epoxy nanocomposite".

Fig. 18 shows the fractional change in electrical resistance (ΔR/R0) of the CNT networks with random and aligned nanotubes distributions as a function of applied strains. From Fig. 18, it can be observed that the nanocomposite with random CNT distribution shows higher strain sensitivity (k = 34.2) comparing nanocomposite with aligned nanotubes (k = 26.0, k = 21.1).

This means that although the magnetized nanocomposites have higher electrical conductivity; the nanocomposites with random nanotube distribution are more sensitive to strain.

Conclusions

The effect of shear mixing parameters (for CNT/epoxy suspension preparation) and CNT concentration on electric conductivity and tensile strength of CNT/epoxy nanocomposites were studied experimentally. For this purpose, composite samples were produced, characterized and tested. Optical microscopy was used to study the morphology of CNT/epoxy suspensions. Three indicators (A_{50}, A_{90} and A_{occ}) were defined respect to CNT clusters surface area and used to analyze the dispersion state of CNT clusters.

The effectiveness of the process parameters on electric conductivity and tensile strength of nanocomposite was studied using ANOVA and two regression models were established to predict electric conductivity and tensile strength of the CNT/epoxy nanocomposites. The robustness and accuracy of the models were verified by implementing verification tests. The effect of fabrication parameters on strain sensing properties of the nanocomposites was also investigated by citing sensitivity, bias and nonlinearity of the prepared nanocomposites.

With account for the results discussed above, the following main conclusions can be drawn about the effect of shear mixing parameters and CNT concentration on electric conductivity, tensile strength and strain sensing properties of CNT/epoxy nanocomposites:

- The suspension dispersion homogeneity is not affected by mixing time at low CNT concentration (0.2 wt%). However, for high concentrated samples (0.5 wt%) using higher mixing speed with longer periods of mixing time is resulted in finer structure (lower A_{50} and A_{90} values and higher A_{occ}).
- Electric conductivity of the high concentrated nanocomposites is strongly affected by mixing parameters. On the other hand, mixing parameters do not show significant effect on electric conductivity when the CNT loading was set to its low value.
- Tensile strength of the nanocomposites those are prepared using low mixing speed, regardless of mixing time and CNT concentration is significantly lower than the strength of not reinforced epoxy.
- Strain sensory behavior of the nanocomposite gauges containing higher amount of CNTs is not affected by mixing speed and time. Respect to the obtained high gauge sensitivity with acceptable bias and nonlinearity, the nanocomposites fabricated by dispersing of low amount of CNT (0.2 wt%) with high mixing speed and long mixing time are more suitable for strain sensing applications.
- The electrical properties of nanocomposites are increased near two times by subjecting CNT-epoxy suspension in a magnetic field of 0.2 T during curing cycle. The following morphological study of theses samples show that CNTs have been aligned to the direction of the magnetic field.
- Simulation results demonstrate that the electrical conductivity of nanocomposites with aligned nanotubes is around 1.5 times greater

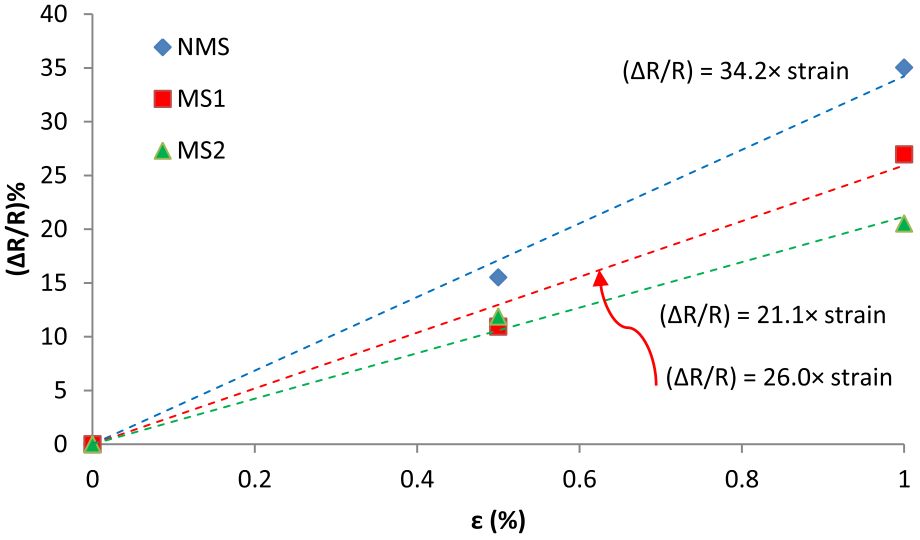

Fig. 18. Fractional change in electrical resistance (ΔR/R0) of the CNT network model under tensile strain. The model assumed that N = 250, $L_{CNT} = 1.5\,\mu m$, $R_t = 100\,k\Omega$, $R_{jct} = 1\,k\Omega$.

than those have randomly distributed nanotubes in their microstructures. Despite this improvement in electrical conductivity, the variation in electrical resistance was more pronounced for randomly distributed microstructures. Strain sensitivity factor (Gauge factor) as high as 35 and 27 were predicted for nanocomposites made from random and aligned nanotube microstructures, respectively.

Acknowledgment

This study was supported by Middle East Technical University Office of Scientific Research Projects Coordination (BAP-03-02-2015-005) through the project “Manufacturing of electrical conductive pathways in fiber reinforced composites via micro vascular channels”.

Appendix

In ANOVA, significance of each term is evaluated using Fisher's variance ratio (F-value) and probability value (P-value) which are calculated based on Degrees of freedom (DF), sequential sums of squares (Seq SS), adjusted sums of squares (Adj SS), the adjusted mean square (Adj MS) [41]. P-value is defined as probability against null hypothesis which is denoted as H0 and stated as “Treatment does not have significant effect on response”. Terms with p-values less than significance level threshold ($\alpha = 0.05$) are considered as significant terms.

The analysis of variance on conductivity data (Table 5) is shown in Table 8. The respective regression model that fits the experimental data can be represented as:

$$\sigma = 2.360 - 0.001N - 0.040T - 8.234W + (1.0 \times 10^{-5})N^2 + (6.0 \times 10^{-5})T^2 + 7.738W^2 + (2.0 \times 10^{-5})N.\ T + (0.003)N.\ W + (0.072)T.\ W \quad (18)$$

Table 8
Analysis of variance on conductivity (S/m), the analysis was done on uncoded units.

Source	DF	Adj SS	Adj MS	F	P
Regression	9	515.953	57.328	6.48	0.004
Linear	3	297.805	99.268	11.22	0.002
Mixing speed (rpm)	1	58.864	58.864	6.65	0.027
Mixing time (min)	1	47.211	47.211	5.33	0.044
Concentration (wt%)	1	191.730	191.730	21.66	0.001
Quadratic	3	33.966	11.322	1.28	0.334
Mixing speed (rpm) * mixing speed (rpm)	1	1.368	1.368	0.15	0.702
Mixing time (min) * mixing time (min)	1	0.533	0.533	0.06	0.811
Concentration (wt %) * concentration (wt%)	1	8.938	8.938	1.01	0.339
Interaction	3	184.181	61.394	6.94	0.008
Mixing speed (rpm) * mixing time (min)	1	62.519	62.519	7.06	0.024
Mixing speed (rpm) * concentration (wt%)	1	70.496	70.496	7.96	0.018
Mixing time (min) * concentration (wt%)	1	51.167	51.167	5.78	0.037
Residual Error	10	88.514	8.851		
Lack-of-Fit	5	87.599	17.520	95.74	< 0.001
Total	19	604.466			

Table 9
Electric conductivity and transformed conductivity of CNT-epoxy nanocomposite samples.

Run order	sample	Electric conductivity $\times 10^{-3}$ (S/m)	$\sigma_t \times 10^{-3}$ (S/m)
1	500N10T20W	0.198	−1.6195
2	2000N10T20W	0.102	−2.2828
3	500N60T20W	0.250	−1.3863
4	2000N60T20W	0.278	−1.2801
5	500N10T50W	4.230	1.4422
6	2000N10T50W	4.950	1.5994
7	500N60T50W	3.340	1.2060
8	2000N60T50W	26.300	3.2696
9	500N35T35W	1.660	0.5068
10	2000N35T35W	2.310	0.8372
11	1250N10T35W	1.200	0.1823
12	1250N60T35W	2.240	0.8064
13	1250N35T20W	0.185	−1.6874
14	1250N35T50W	5.980	1.7884
15	1250N35T35W	1.460	0.3784
16	1250N35T35W	2.140	0.7608
17	1250N35T35W	2.500	0.9163
18	1250N35T35W	2.300	0.8329
19	1250N35T35W	2.680	0.9858
20	1250N35T35W	2.420	0.8838

Table 10
Analysis of Variance on transformed conductivity data (σ_t).

Source	DF	Adj SS	Adj MS	F	P
Regression	9	36.0541	4.0060	79.33	< 0.001
Linear	3	32.3238	10.7746	213.38	< 0.001
Mixing speed (rpm)	1	0.3976	0.3976	7.87	0.019
Mixing time (min)	1	1.0850	1.0850	21.49	0.001
Concentration (wt%)	1	30.8412	30.8412	610.77	0.000
Quadratic	3	1.8658	0.6219	12.32	0.001
Mixing speed (rpm) * mixing speed (rpm)	1	0.0087	0.0087	0.17	0.686
Mixing time (min) * mixing time (min)	1	0.0405	0.0405	0.80	0.392
Concentration (wt %) * concentration (wt%)	1	0.8784	0.8784	17.40	0.002
Interaction	3	1.8645	0.6215	12.31	0.001
Mixing speed (rpm) * mixing time (min)	1	0.8950	0.8950	17.72	0.002
Mixing speed (rpm) * concentration (wt %)	1	0.9646	0.9646	19.10	0.001
Mixing time (min) * concentration (wt%)	1	0.0049	0.0049	0.10	0.762
Residual Error	10	0.5050	0.0505		
Lack-of-Fit	5	0.2698	0.0540	1.15	0.442
Total	19	36.5591			
R^2 = 98.6%	R^2_{pred} = 97.4%			R^2_{adj} = 87.6%	

Based on results of Table 8 there is a significant lack-of-fit in regression model (Eq. (18)), indicating this regression model is not able to describe the functional relationship between experimental factors and electric conductivity.

The Lack-of-fit issue can be resolved by using transformation of the response. The Box-Cox transformation [52] is the most commonly used technique at which an appropriate exponent (Lambda) is used to transform response data. The Box-Cox transformation is defined as:

$$y_i^{(\lambda)} = \begin{cases} \frac{y_i^{\lambda} - 1}{\lambda}, & \lambda \neq 0 \\ \ln(y_i), & \lambda = 0 \end{cases} \tag{19}$$

where y_i is original data and $y_i^{(\lambda)}$ is transformed data. The optimal value for exponent Lambda was found by analyzing data in Minitab and then response data were transformed using Eq. (20) by specifying Lambda equals to zero.

$$\sigma_t = \ln(\sigma) \tag{20}$$

where σ is the electric conductivity and σ_t is the transformed electric conductivity. The transformed electric conductivities are represented in Table 9.

Table 10 presents analysis of variance on transformed conductivity (σ_t) considering main factors, quadratic terms and their interactions. Considering the calculated p-values, quadratic terms of mixing speed (0.824), mixing time (0.485) and interaction of mixing time and concentration (0.168) have no significant effect on transformed electric conductivity.

These terms are removed from the model and respective analysis of variance is represented in Table 11. Mixing time is shown to have no

Table 11
Analysis of variance for transformed conductivity, some predictors have been eliminated.

Source	DF	Adj SS	Adj MS	F	P
Regression	6	36.0084	6.0014	141.67	0.000
Linear	3	32.3238	10.7746	254.35	0.000
Mixing speed (rpm)	1	0.3976	0.3976	9.39	0.009
Mixing time (min)	1	1.0850	1.0850	25.61	0.000
Concentration (wt%)	1	30.8412	30.8412	728.05	0.000
Quadratic	1	1.8249	1.8249	43.08	0.000
Concentration (wt %) * concentration (wt%)	1	1.8249	1.8249	43.08	0.000
Interaction	2	1.8596	0.9298	21.95	0.000
Mixing speed (rpm) * mixing time (min)	1	0.8950	0.8950	21.13	0.001
Mixing speed (rpm) * concentration (wt%)	1	0.9646	0.9646	22.77	0.000
Residual Error	13	0.5507	0.0424		
Lack-of-Fit	8	0.3156	0.0394	0.84	0.608
Total	19	36.5591			
R^2 = 98.5%	R^2_{pred} = 97.8%			R^2_{adj} = 94.6%	

Table 12
Analysis of variance on tensile strength of CNT/epoxy nanocomposite.

Source	DF	Seq SS	Adj SS	Adj MS	F	P
Regression	9	1707.6	1707.6	189.733	6.48	0.004
Linear	3	1537.56	128.08	42.694	1.46	0.284
Mixing speed (rpm)	1	1480.28	69.98	69.981	2.39	0.153
Mixing time (min)	1	36.74	4.53	4.525	0.15	0.702
Concentration (wt%)	1	20.54	7.21	7.211	0.25	0.63
Quadratic	3	160.86	160.86	53.621	1.83	0.205
Mixing speed (rpm) * mixing speed (rpm)	1	128.36	21.26	21.258	0.73	0.414
Mixing time (min) * mixing time (min)	1	18.21	6.44	6.44	0.22	0.649
Concentration (wt%) * concentration (wt%)	1	14.3	14.3	14.299	0.49	0.5
Interaction	3	9.18	9.18	3.059	0.1	0.956
Mixing speed (rpm) * mixing time (min)	1	5.84	5.84	5.837	0.2	0.665
Mixing speed (rpm) * concentration (wt%)	1	2.92	2.92	2.92	0.1	0.759
Mixing time (min) * concentration (wt%)	1	0.42	0.42	0.42	0.01	0.907
Residual Error	10	292.59	292.59	29.259		
Lack-of-Fit	5	235.38	235.38	47.076	4.11	0.073
Total	5	57.21	57.21	11.442		
$R^2 = 85.37\%$	$R^2_{pred} = 0.00\%$			$R^2_{adj} = 72.21\%$		

Table 13
Analysis of Variance on tensile strength, some predictors have been eliminated.

Source	DF	Seq SS	Adj SS	Adj MS	F	P
Regression	4	1655.98	1655.98	414	18.04	< 0.001
Linear	3	1537.56	1618.63	539.54	23.51	< 0.001
Mixing speed (rpm)	1	1480.28	1480.28	1480.28	64.51	< 0.001
Mixing time (min)	1	36.74	36.74	36.74	1.6	0.225
Concentration (wt%)	1	20.54	101.61	101.61	4.43	0.053
Quadratic	1	118.42	118.42	118.42	5.16	0.038
Concentration (wt %) * concentration (wt%)	1	118.42	118.42	118.42	5.16	0.038
Residual Error	15	344.21	344.21	22.95		
Lack-of-Fit	10	287	287	28.7	2.51	0.161
Total	5	57.21	57.21	11.44		
$R^2 = 82.8\%$	$R^2_{pred} = 68.3\%$			$R^2_{adj} = 78.2\%$		

significant effect on electric conductivity as an individual parameter. However, the interaction of mixing time and mixing speed has significant effect on composite conductivity as the calculated p-value is less than the significance level threshold ($\alpha = 0.05$).

The regression model that fits the experimental data based on the results of Table 11 can be represented as:

$$\sigma_t = -5.341 - 0.001N - 0.009T + 26.65W - 26.85W^2 + (0.309 \times 10^{-2})N.\ T + (0.003)N.\ W \quad (21)$$

The adjusted R^2_{adj} (which denotes how successfully the experimental data fits the model) for the regression model has been calculated as 94.6%, indicating the improvement in the fit by the logarithmic model.

Analysis of variance on tensile strength data is shown in Table 12. Based on results, quadratic and interaction terms have no significant effect on strength. Considering calculated P-values, no significant terms are removed and respective analysis of variance on tensile test results considering the main factors and quadratic term of concentration is presented in Table 13. This analyze continues up to obtain the highest R^2_{adj}.

References

[1] Loos MR, Coelho LAF, Pezzin SH, Amico SC. Effect of carbon nanotubes addition on the mechanical and thermal properties of epoxy matrices. Mater Res 2008;11:347–52.

[2] Yamamoto N, Guzman de Villoria R, Wardle BL. Electrical and thermal property enhancement of fiber-reinforced polymer laminate composites through controlled implementation of multi-walled carbon nanotubes. Compos Sci Technol 2012;72:2009–15. https://doi.org/10.1016/j.compscitech.2012.09.006.

[3] Ma P-C, Liu M-Y, Zhang H, Wang S-Q, Wang R, Wang K, et al. Enhanced electrical conductivity of nanocomposites containing hybrid fillers of carbon nanotubes and carbon black. ACS Appl Mater Interfaces 2009;1:1090–6. https://doi.org/10.1021/am9000503.

[4] Wen X, Wang Y, Gong J, Liu J, Tian N, Wang Y, et al. Thermal and flammability properties of polypropylene/carbon black nanocomposites. Polym Degrad Stab 2012;97:793–801. https://doi.org/10.1016/j.polymdegradstab.2012.01.031.

[5] Huang G, Wang S, Song P, Wu C, Chen S, Wang X. Combination effect of carbon nanotubes with graphene on intumescent flame-retardant polypropylene nanocomposites. Compos Part A 2014;59:18–25. https://doi.org/10.1016/j.compositesa.2013.12.010.

[6] Sofocleous K, Drakonakis VM, Ogin SL, Doumanidis C. The influence of carbon nanotubes and shape memory alloy wires to controlled impact resistance of polymer composites. J Compos Mater 2017;51:273–85. https://doi.org/10.1177/0021998316640594.

[7] Parvaneh V, Shariati M. Experimental analysis of the low cycle fatigue of a spray-coated layered multi-walled carbon nanotubes/polyvinyl chloride nanocomposite. J Compos Mater 2016;50:1555–62. https://doi.org/10.1177/0021998315595112.

[8] Tang L-C, Wan Y-J, Peng K, Pei Y-B, Wu L-B, Chen L-M, et al. Fracture toughness and electrical conductivity of epoxy composites filled with carbon nanotubes and spherical particles. Compos Part A 2013;45:95–101. https://doi.org/10.1016/j.compositesa.2012.09.012.

[9] Zhou YX, Wu PX, Cheng Z, Ingram J, Jeelani S. Improvement in electrical, thermal and mechanical properties of epoxy by filling carbon nanotube. Express Polym Lett

2008;2:40–8. https://doi.org/10.3144/expresspolymlett.2008.6.
[10] Siddiqui NA, Li EL, Sham M, Zhong B, Lin S, Mäder E, et al. Tensile strength of glass fibres with carbon nanotube – epoxy nanocomposite coating: effects of CNT morphology and dispersion state. Compos Part A 2010;41:539–48. https://doi.org/10.1016/j.compositesa.2009.12.011.
[11] Ma PC, Siddiqui NA, Marom G, Kim JK. Dispersion and functionalization of carbon nanotubes for polymer-based nanocomposites: a review. Compos Part A 2010;41:1345–67. https://doi.org/10.1016/j.compositesa.2010.07.003.
[12] Kim S, Lee WI, Park CH. Assessment of carbon nanotube dispersion and mechanical property of epoxy nanocomposites by curing reaction heat measurement. J Reinf Plast Compos 2016. https://doi.org/10.1177/0731684415613704.
[13] Overbeck A, Linke S, Kwade A, Schilde C, Schl M. Thermal, mechanical and electrical properties of highly loaded CNT-epoxy composites e A model for the electric conductivity. Compos Sci Technol 2015;117:183–90. https://doi.org/10.1016/j.compscitech.2015.06.013.
[14] Bauhofer W, Kovacs JZ. A review and analysis of electrical percolation in carbon nanotube polymer composites. Compos Sci Technol 2009;69:1486–98. https://doi.org/10.1016/j.compscitech.2008.06.018.
[15] Xie X, Mai Y, Zhou X. Dispersion and alignment of carbon nanotubes in polymer matrix: a review. Mater Sci Eng A 2006;49:89–112. https://doi.org/10.1016/j.mser.2005.04.002.
[16] Sandler J, Shaffer MSP, Prasse T, Bauhofer W, Schulte K, Windle AH. Development of a dispersion process for carbon nanotubes in an epoxy matrix and the resulting electrical properties. Polymer (Guildf) 1999;40:5967–71.
[17] Guru K, Mishra SB, Shukla KK. Effect of temperature and functionalization on the interfacial properties of CNT reinforced nanocomposites. Appl Surf Sci 2015;349:59–65. https://doi.org/10.1016/j.apsusc.2015.04.196.
[18] Cha J, Jin S, Hun J, Soo C, Jin H, Hyung S. Functionalization of carbon nanotubes for fabrication of CNT/epoxy nanocomposites. JMADE 2016;95:1–8. https://doi.org/10.1016/j.matdes.2016.01.077.
[19] Fan Z, Hsiao K-T, Advani SG. Experimental investigation of dispersion during flow of multi-walled carbon nanotube/polymer suspension in fibrous porous media. Carbon N Y 2004;42:871–6. https://doi.org/10.1016/j.carbon.2004.01.067.
[20] Geng Y, Liu MY, Li J, Shi XM, Kim JK. Effects of surfactant treatment on mechanical and electrical properties of CNT/epoxy nanocomposites. Compos Part A 2008;39:1876–83. https://doi.org/10.1016/j.compositesa.2008.09.009.
[21] Pillai S, Ray S. Epoxy-based carbon nanotubes reinforced composites. Adv Nanocomposites – Synth Charact Ind Appl Ed by Dr Boreddy Reddy 2011:727.
[22] Yum SH, Roh JU, Park JM, Park JK, Kim SM, Lee W Il. Assessment of particle distribution in particle-containing composite materials using an electron probe microanalyzer. Compos Sci Technol 2013;82:38–46. https://doi.org/10.1016/j.compscitech.2013.04.008.
[23] Castellino M, Chiolerio A, Shahzad MI, Jagdale PV, Tagliaferro A. Electrical conductivity phenomena in an epoxy resin–carbon-based materials composite. Compos Part A 2014;61:108–14. https://doi.org/10.1016/j.compositesa.2014.02.012.
[24] Hu N, Masuda Z, Yamamoto G, Fukunaga H. Effect of fabrication process on electrical properties of polymer/multi-wall carbon nanotube nanocomposites. Compos Part A 2008;39:893–903. https://doi.org/10.1016/j.compositesa.2008.01.002.
[25] Kovacs JZ, Velagala BS, Schulte K, Bauhofer W. Two percolation thresholds in carbon nanotube epoxy composites. Compos Sci Technol 2007;67:922–8. https://doi.org/10.1016/j.compscitech.2006.02.037.
[26] Moaseri E, Karimi M, Baniadam M, Maghrebi M. Improvements in mechanical properties of multi-walled carbon nanotube-reinforced epoxy composites through novel magnetic-assisted method for alignment of carbon nanotubes. Compos Part A 2014;64:228–33. https://doi.org/10.1016/j.compositesa.2014.05.014.
[27] Lipert K, Ritschel M, Leonhardt A, Krupskaya Y, Büchner B, Klingeler R. Magnetic properties of carbon nanotubes with and without catalyst. J Phys Conf Ser 2010;200:72061.
[28] Andreev AS, Kazakova MA, Ishchenko AV, Selyutin AG, Lapina OB, Kuznetsov VL, et al. Magnetic and dielectric properties of carbon nanotubes with embedded cobalt nanoparticles. Carbon N Y 2017;114:39–49. https://doi.org/10.1016/j.carbon.2016.11.070.
[29] Ma C, Liu H, Du X, Mach L, Xu F, Mai Y. Fracture resistance, thermal and electrical properties of epoxy composites containing aligned carbon nanotubes by low magnetic field. Compos Sci Technol 2015;114:126–35. https://doi.org/10.1016/j.compscitech.2015.04.007.
[30] Arguin M, Sirois F, Therriault D, Arguin M. Electric field induced alignment of multiwalled carbon nanotubes in polymers and multiscale composites electric field induced alignment of multiwalled carbon nanotubes in polymers and multiscale composites. Adv Manuf Polym Compos Sci 2015;0340. https://doi.org/10.1179/2055035914Y.0000000003.
[31] Wichmann MHG, Meyer LO, Schulte K. Load and health monitoring in glass fibre reinforced composites with an electrically conductive nanocomposite epoxy matrix. Compos Sci Technol 2008;68:1886–94. https://doi.org/10.1016/j.compscitech.2008.01.001.
[32] Grammatikos SA, Paipetis AS. On the electrical properties of multi scale reinforced composites for damage accumulation monitoring. Compos Part B 2012;43:2687–96. https://doi.org/10.1016/j.compositesb.2012.01.077.
[33] Knite M, Teteris V, Kiploka A, Kaupuzs J. Polyisoprene-carbon black nanocomposites as tensile strain and pressure sensor materials. Sens Actuators, A 2004;110:142–9. https://doi.org/10.1016/j.sna.2003.08.006.
[34] Ramalingame R, Udhayakumar N, Torres R, Neckel IT, Müller C, Kanoun O. MWCNT-PDMS nanocomposite based flexible multifunctional sensor for health monitoring. Procedia Eng 2016;168:1775–8. https://doi.org/10.1016/j.proeng.2017.02.003.
[35] Kang I, Schulz MJ, Kim JH, Shanov V, Shi D. A carbon nanotube strain sensor for structural health monitoring. Smart Mater Struct 2006;15:737.
[36] Ma P, Siddiqui NA, Marom G, Kim J. Dispersion and functionalization of carbon nanotubes for polymer-based nanocomposites: a review. Compos Part A 2010;41:1345–67. https://doi.org/10.1016/j.compositesa.2010.07.003.
[37] Menna C, Bakis CE, Prota A. Effect of nanofiller length and orientation distributions on Mode I fracture toughness of unidirectional fiber composites. J Compos Mater 2016;50:1331–52. https://doi.org/10.1177/0021998315590865.
[38] Kumaresan T, Nere NK, Joshi JB. Effect of internals on the flow pattern and mixing in stirred tanks. Ind Eng Chem Res 2005;44:9951–61. https://doi.org/10.1021/ie0503848.
[39] Jirout T, Rieger F. Impeller design for mixing of suspensions. Chem Eng Res Des 2011;89:1144–51. https://doi.org/10.1016/j.cherd.2010.12.005.
[40] Paul EL, Atiemo-obeng VA, Kresta SM. Handbook of industrial mixing Edited by. n.d.
[41] Montgomery DC. Design and analysis of experiments. John Wiley & Sons; 2006.
[42] Schneider CA, Rasband WS, Eliceiri KW. NIH Image to ImageJ: 25 years of image analysis. Nat Methods 2012;9:671–5.
[43] Schroder DK. Semiconductor material and device characterization. Wiley-Interscience; 2006.
[44] Ashkan Behnam AU. Computational study of geometry-dependent resistivity scaling in single-walled carbon nanotube films. Phys Rev 2007. https://doi.org/10.1103/PhysRevB.75.125432.
[45] Lee BM, Loh KJ. A 2D percolation-based model for characterizing the piezoresistivity of carbon nanotube-based films. J Mater Sci 2015;50:2973–83. https://doi.org/10.1007/s10853-015-8862-y.
[46] Lee BM, Loh KJ. Carbon nanotube thin fi lm strain sensors: comparison between experimental tests and numerical simulations. Nanotechnology 2017;28:155502https://doi.org/10.1088/1361-6528/aa6382.
[47] Amini A, Bahreyni B. Behavioral model for electrical response and strain sensitivity of nanotube-based nanocomposite materials. J Vac Sci Technol B 2012;30. https://doi.org/10.1116/1.3691654.
[48] Singh AK, Harsha SP, Parashar A. Finite Element Analysis of CNT reinforced epoxy composite due to thermo-mechanical loading. Procedia Technol 2016;23:138–43. https://doi.org/10.1016/j.protcy.2016.03.009.
[49] Korayem AH, Barati MR, Simon GP, Zhao XL, Duan WH. Reinforcing brittle and ductile epoxy matrices using carbon nanotubes masterbatch. Compos Part A 2014;61:126–33. https://doi.org/10.1016/j.compositesa.2014.02.016.
[50] Häntzsche E, Matthes A, Nocke A, Cherif C. Physical characteristics of carbon fiber based strain sensors for structural-health monitoring of textile-reinforced thermoplastic composites depending on the textile technological integration process. Sens Actuators, A 2013;203:189–203. https://doi.org/10.1016/j.sna.2013.08.045.
[51] Pyzdek T, Keller PA. Quality engineering handbook. Taylor & Francis; 2003.
[52] Kowalski SM, Montgomery DC. Design and analysis of experiments: MINITAB companion. J. Wiley & Sons 2011.